crystals

MDPI

Article

Semipolar $\{20\bar{2}1\}$ GaN Edge-Emitting Laser Diode on Epitaxial Lateral Overgrown Wing

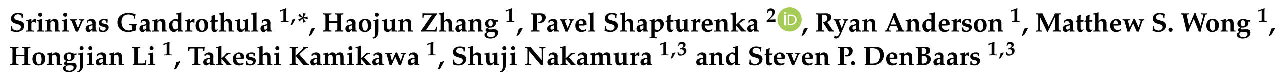
Srinivas Gandrothula [1,*], Haojun Zhang [1], Pavel Shapturenka [2], Ryan Anderson [1], Matthew S. Wong [1], Hongjian Li [1], Takeshi Kamikawa [1], Shuji Nakamura [1,3] and Steven P. DenBaars [1,3]

[1] Materials Department, University of California, Santa Barbara, CA 93106, USA; hzhang@ucsb.edu (H.Z.); randerson@ucsb.edu (R.A.); m_wong@ucsb.edu (M.S.W.); hongjianli@ucsb.edu (H.L.); takeshi_kamikawa@ucsb.edu (T.K.); snakamura@ucsb.edu (S.N.); spdenbaars@ucsb.edu (S.P.D.)
[2] Department of Chemical Engineering, University of California, Santa Barbara, CA 93106, USA; pavel@ucsb.edu
[3] Department of Electrical and Computer Engineering, University of California, Santa Barbara, CA 93106, USA
* Correspondence: sgandrothula@ucsb.edu

Abstract: Edge-emitting laser diodes (LDs) were fabricated on a reduced dislocation density epitaxial lateral overgrown (ELO) wing of a semipolar $\{20\bar{2}1\}$ GaN substrate, termed an ELO wing LD. Two types of facet feasibility studies were conducted: (1) "handmade" facets, wherein lifted-off ELO wing LDs were cleaved manually, and (2) facets formed on wafers through reactive ion etching (RIE). Pulsed operation electrical and optical measurements confirmed the laser action in the RIE facet LDs with a threshold current of ~19 kAcm^{-2} and maximum light output power of 20 mW from a single uncoated facet. Handmade facet devices showed spontaneous, LED-like emission, confirming device layers remain intact after mechanical liftoff.

Keywords: GaN; semipolar; $\{20\bar{2}1\}$; epitaxial lateral overgrowth; laser diode; defects; recycling; nitride semiconductor

Citation: Gandrothula, S.; Zhang, H.; Shapturenka, P.; Anderson, R.; Wong, M.S.; Li, H.; Kamikawa, T.; Nakamura, S.; DenBaars, S.P. Semipolar $\{20\bar{2}1\}$ GaN Edge-Emitting Laser Diode on Epitaxial Lateral Overgrown Wing. *Crystals* **2021**, *11*, 1563. https://doi.org/10.3390/cryst11121563

Academic Editors: Haiding Sun, Bharat Jalan, Shibing Long, Yuhao Zhang, Rajendra Singh, Xuelin Yang, Yuji Zhao Bin Liu and M. Ajmal Khan

Received: 12 November 2021
Accepted: 13 December 2021
Published: 14 December 2021

Publisher's Note: MDPI stays neutral with regard to jurisdictional claims in published maps and institutional affiliations.

Copyright: © 2021 by the authors. Licensee MDPI, Basel, Switzerland. This article is an open access article distributed under the terms and conditions of the Creative Commons Attribution (CC BY) license (https://creativecommons.org/licenses/by/4.0/).

1. Introduction

The development of (Al,Ga,In) nitride-based semiconductor technology has shown continuous progress and promise since the first demonstration of blue semiconductor laser diodes (LDs) in the 1990s [1,2]. After the great success of blue-light emitting diodes (LEDs) in lighting applications earned him the 2014 Nobel Prize in Physics, Shuji Nakamura turned his attention to LD-based applications [3]. InGaN/GaN LDs offer more power per chip area, much higher brightness, and no efficiency drop above threshold [4]. Moreover, InGaN/GaN blue and green LDs are the subject of many applications, including optical storage systems, projectors, laser lighting, visible light communication, and high-intensity automobile head lamps [5–9]. To date, InGaN/GaN LDs have been mainly fabricated on {0001}-oriented c-plane GaN substrates due to their matured epitaxy, easily cleaved crystal facets, substrate availability, size, and price [10,11]. However, the decreasing efficiencies of {0001}-oriented (AlGaIn) nitride-based light emitters with increasing emission wavelengths, along with limited modulation speed and poor wall-plug efficiency, remain the subject of ongoing investigation. This is in part due to the strain-induced piezoelectric fields at InGaN/GaN {0001} heterointerfaces, which result in a low quantum efficiency due to electron–hole wavefunction separation in InGaN quantum wells, the so-called quantum-confined Stark effect (QCSE) [12,13]. QCSE-induced electron–hole wavefunction separation reduces the oscillator strength of optical transitions, resulting in a reduced radiative recombination rate and poor device performance.

Accordingly, semi- and non-polar-oriented GaN surface planes are studied as attractive alternative growth substrates to achieve higher electron–hole wavefunction overlap for increased radiative recombination efficiency and higher material gain [14–20]. However, high substrate cost, supply, and size limitations preclude the full realization of the

market potential of semi-and non-polar LDs. To address these limitations, we propose a new approach combining ELO and a robust peeling method for semi- and non-polar optical devices ([21–28], patent applications (i)–(xxx)). The feasibility of this new approach was studied for various devices such as non-polar LDs [21], n-side-distributed Bragg reflectors [23], and semipolar µLEDs [24]. Briefly, the process by which we may lower the commercialization hurdle consists of (1) utilizing ELO on expensive, free-standing GaN substrates for optical device fabrication, (2) removing the devices from the substrate, and (3) reusing the expensive substrate. This procedure of removing GaN thin films can also be beneficial in the bonding and integration of visible wavelength devices onto the Si photonics platform [29]. While earlier work reported a functional $\{10\bar{1}0\}$-non-polar LD with a laser ridge on an ELO open window [21], non-polar crystalline planes limit the attainable indium content. Long-wavelength emission therefore demands the use of semipolar crystalline planes, such as the semipolar $\{20\bar{2}1\}$ orientation [30]. It is therefore expected that an extension of the ELO LD and the removal of the workflow to semipolar GaN substrates will meet this need. Moreover, coupled with the wider wings and reduced defect densities achievable with such planes [22,24], semipolar ELO may also enhance device lifetimes and lower the threshold current of ELO-templated laser ridges [31]. We earlier reported reduced threading dislocations on the ELO wings of $\{20\bar{2}1\}$ crystalline plane [24]. As such, the following study features laser diodes formed on the wings of the $\{20\bar{2}1\}$ crystalline plane, which allows for indium incorporation at higher temperatures for higher crystal quality growth of the quantum wells, assuming a similar reduction in threading dislocations.

2. Materials and Methods

The ELO wing LD concept is schematically represented in Figure 1. As shown in Figure 1a, a patterned semipolar $\{20\bar{2}1\}$ substrate (~10 × 5 mm) was prepared for base ELO layer growth. A 1000-nanometer-thick SiO_2 as ELO mask was blanket-deposited on the $\{20\bar{2}1\}$ substrate using plasma-enhanced chemical vapor deposition (PECVD) and patterned by opening window stripes parallel to the $<\bar{1}014>$- axis (projection of c-axis on the $\{20\bar{2}1\}$ surface), each having dimensions of 5 µm × 3 mm periodically arrayed 55 µm breadthwise. The SiO_2-patterned substrate was then inserted into a metal–organic chemical vapor deposition (MOCVD) reactor; unintentionally doped (UID) GaN ELO layers were grown with 10 slm of ammonia (NH_3) and 12 sccm of trimethylgallium (TMG) as sources and 10 slm of H_2 as the carrier gas at a reactor pressure of 100 torr and a temperature of 1210 °C. UID-GaN layers were then grown epitaxially from the patterned open windows of the $\{20\bar{2}1\}$ substrate and proceeded to form wings laterally over the SiO_2 ELO mask. UID-GaN layer growth was stopped before coalescence with the neighboring ELO layers. In approximately 400 min UID-GaN ELO layers achieved a final epitaxial layer thicknesses of ~25 µm and wing widths of ~17 µm. The SiO_2 ELO mask was dissolved in hydrofluoric acid (HF) followed by DI water rinsing and then reintroduced into the MOCVD reactor for standard laser structure epitaxy (Figure 1d). The laser structure comprised a 1.2-micrometer thick lower Si-doped GaN cladding layer, a 65-nanometer thick Si-doped $In_{0.06}Ga_{0.94}N$ lower waveguide, a two-period multi-quantum well (MQW) structure with 3/7-nanometer InGaN well/GaN barrier, a 20-nanometer-micrometer-thick p-$Al_{0.28}Ga_{0.72}$ N electron blocking layer (EBL), a 65-micrometer-thick Mg-doped $In_{0.06}Ga_{0.94}N$ upper waveguide, and a 250-nanometer-thick Mg-doped GaN upper cladding layer as previously reported [20]. Epi-wafer electroluminescence (EL) showed an emission wavelength centered at ~426 nm.

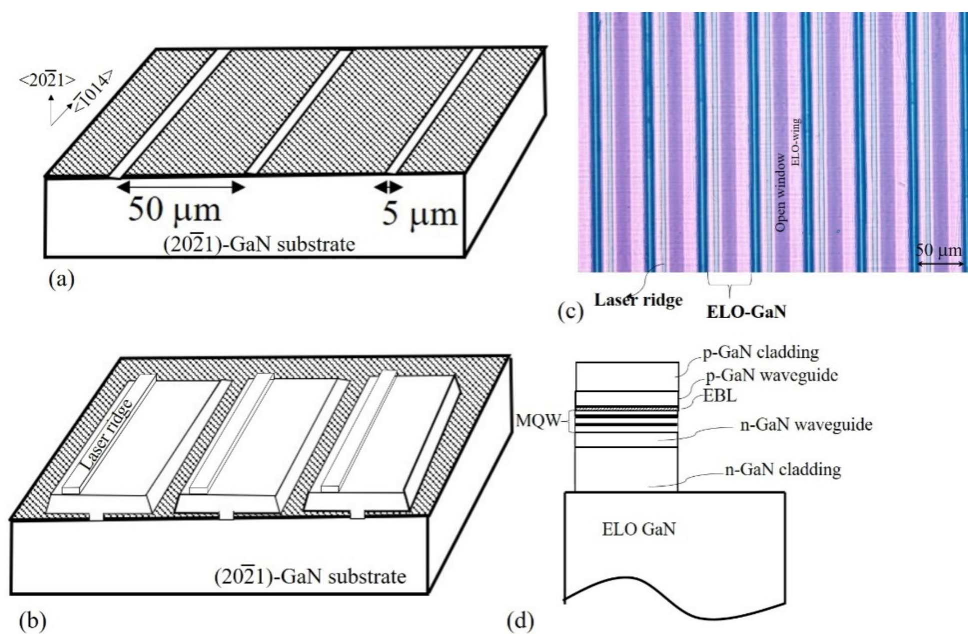

Figure 1. (**a**) SiO_2 mask design on {20$\bar{2}$1 } semipolar GaN substrate, where open windows are 5 µm in width and masked portions are 50 µm in width. (**b**) Bird-view sketch of grown GaN ELO layers from the open window and proposed laser ridge on wing. (**c**) Optical microscope image showing processed LD ridge on ELO wings. (**d**) An illustration showing the laser structure cross-section.

A 15 min, 600 °C furnace activation was performed in ambient air following epitaxial growth to activate Mg dopants. Then, 5-micrometer-wide ridge waveguides were defined using a bilayer photoresist (PR) comprising SPR 220-3.0 as a top layer and a recessed underlayer LOL 2000 as bottom layer on the ELO wings. These were oriented along the 3-millimeter-long ELO open windows, i.e., parallel to the c-axis projection on the {20$\bar{2}$1} surface as indicated in Figure 1b,c. Then, Cl_2 plasma reactive ion etching (RIE) was performed with an etch rate of 110 nm/min on the p-GaN cladding layer. Then, a 300-nanometer-thick SiO_2 layer was deposited by magnetron sputtering. The bilayer PR assists in a self-aligned lift-off process to form the ridge waveguide and insulation between n- and p-electrical pads. Prior to p-contact deposition, a two-fold 5-minute cycle of heated aqua regia immersion (1:3 nitric: hydrochloric acid) was performed, followed by DI water rinse. A 150-nanometer-thick indium tin oxide (ITO) was blanket deposited using e-beam evaporation at a substrate temperature of 250 °C to serve as p-contact and cladding layer. Then, after defining p-contacts, the ITO etched by RIE using $CH_4/H_2/Ar$ (4/20/10 sccm) chemistry at 75 mT of chamber pressure and DC bias of 350 V. Ti/Au (10/300 nm) p-contact pads were deposited using an e-beam system on top of the ITO. Then, the sample was divided into two equal pieces, one used in handmade facet and the other in on-wafer RIE facet studies.

3. Results and Discussion

3.1. Handmade Facet Formation

Serving as the backing for mass transfer, adhesive tape was gently placed on the ELO wing LDs and firmly pressed with a soft roller. The assembly was then introduced into 77K liquid nitrogen bath, where it was left for about two minutes. Next, the tape was slowly removed from the taped device assembly after warming to room temperature, as in Figure 2a [22]. This process separates inverted ELO wing LDs from the growth substrate, i.e., with adhesive tape covering the whole p-pad. Figure 2b shows the removed ELO wing LDs upside down on the adhesive film, with a fresh back surface for n-contact deposition. Accordingly, the n-contact was deposited on the back of the removed ELO layers by the blanket evaporation of Ti/Al/Ni/Au (10/50/100/300 nm) using e-beam

evaporation. Very minimal use of the expensive bulk semipolar {20$\bar{2}$1} substrate was observed using this method, and a 100% transfer yield was achieved owing to the narrow open ELO windows (5 μm wide) [22]. Then, the adhesive tape was immersed in acetone to loosen the attached ELO wing LDs. The loosened LDs were carefully placed on a metal-coated (Ti/Au/In 10/300/1500 nm) Si carrier using a laboratory tweezer in downside p-pad configuration, under microscope inspection. Then, a gentle pinch was imposed on the removed ELO layers at random lengths to fracture the layer ends into facets. We observed an unwanted metal layer hanging around the facet when the ELO layers were fractured from the topside (p-side), so facet fracturing was performed from the backside (n-side) to avoid such abnormality. The fractured LD bars were rearranged on the carrier to the depicted probing configuration shown in Figure 2d. The bars on the carrier can be freely moved without annealing or excessive force for strong metal contact with the carrier. As most of this process was done manually, the yield was drastically reduced. Nonetheless, this method yielded a functional {10$\bar{1}$0} non-polar LD with a laser ridge on the ELO open window and was reported in a prior work [21]. In the {10$\bar{1}$0} non-polar ELO LD, the GaN crystalline geometry allowed easy access to cleavable {0001}-oriented c-planes perpendicular to the ridge length, resulting in near-vertical mirror facets. However, the present {20$\bar{2}$1} semipolar ELO layer did not have an easily cleavable plane, such as abovementioned {0001}-oriented c-planes, or non-polar planes for laser cavity mirror facets perpendicular to the ridge length. In 2009, Sumitomo Electric Ltd. reported cleaved facets such as conventional LDs on semipolar {20$\bar{2}$1} by thinning growth substrates and pressing them against a fracturing blade [15]. We believe that adopting such an industrial protocol would greatly benefit our study; as such, ELO wing LDs should be transferred onto a stiff carrier, saving expensive growth substrates. A few possibilities such as acoustic solution printing [32] or stiff carrier transfer procedures (patent application (xxviii)) will be investigated in further detail in other work. Revisiting the present adhesive tape assembly, Figure 2c shows selected examples of laser bars achieved via manual cleaving cavity lengths of (1) 1800, (2) 1390, (3) 780 and (4) 1072 μm. One of the facets is shown magnified; visible inspection revealed curved cavity ends, indicating non-ideal facet formations. The bars were electrically tested for possible laser operation with the probing scheme shown schematically in Figure 2d.

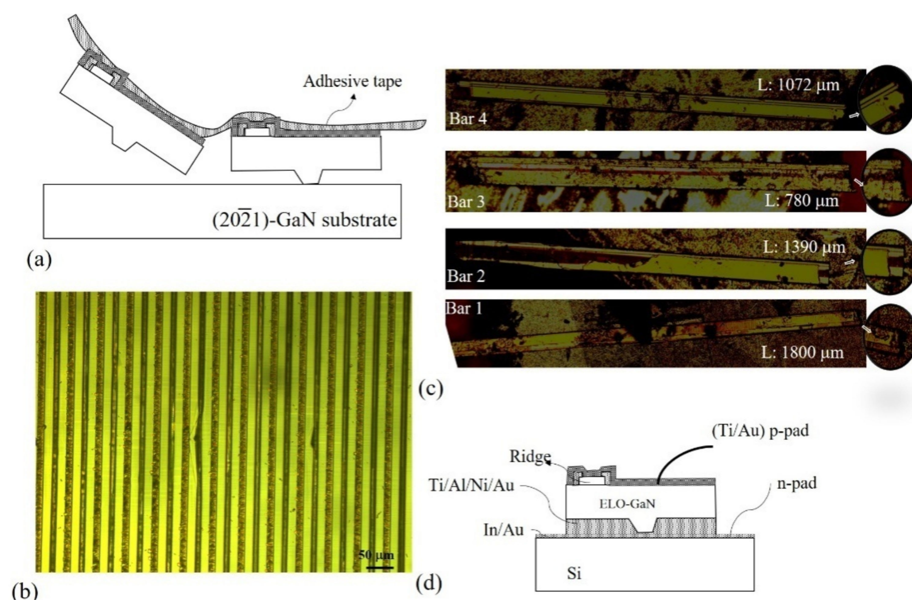

Figure 2. (**a**) Removing illustration of ELO wing LDs with adhesive tape. (**b**) Removed {20$\bar{2}$1} ELO wing LDs on adhesive tape, upside down, before n-contact deposition. (**c**) Random-length ELO wing LDs placed on a Si carrier for measurements, with magnified end facet. (**d**) Probing scheme for type-1 (handmade) facet LDs.

Using pulsed electrical injection, bars were tested with a pulse width of 0.5 µs and 0.5% duty cycle; Figure 3a shows the EL spectra at 10 kAcm^{-2} of all the bars. All spectra showed spontaneous, LED-like emission at pre-liftoff peak emission wavelengths, confirming the intactness of the device layers after mechanical peeling. Out of the measured samples, the spontaneous emission spectrum of bar 4 (1072 µm cavity length) showed a lower full width at half maximum (FWHM) compared to the other bars. Light–current–voltage (L-I-V) characteristics of bar 4 were measured and plotted in Figure 3b. A maximum light output power of 2.3 mW was measured from the fractured facet of bar 4 at a current density of ~27 kAcm^{-2}. Though the line width appears to be narrow for bar 4, the EL spectrum confirms there is no laser action. We concluded that to achieve laser action, we will need to properly optimize the prepared facets and have better control of the cavity length. The current density was calculated by dividing the injected current with the area of the ridge waveguide. Minimum lateral current diffusion was assumed and expected, owing to the etching and poor inherent lateral conductivity of the p-GaN layer. In this probing scheme, the bar n-pad was not in firm contact with the carrier metal; only the p-probe force pressed against the Si carrier provides contact area for n-pad current injection, thereby lacking a proper thermal sink. Therefore, the sample was only operated under pulsed operation, where heating is not a serious concern. Additionally, some residue from the adhesive tape may still be an issue in the sample preparation for this type. Taken collectively, the above device limitations increased the voltage of the measurement.

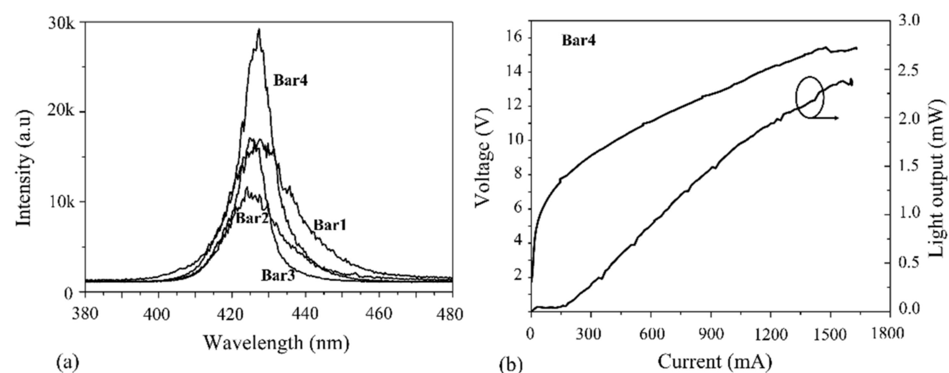

Figure 3. (**a**) EL spectrum at 10 kAcm^{-2} current density for the selected bars shown in Figure 2b. (**b**) L-I-V measurement data for bar 4 under pulsed operation.

3.2. On-Wafer RIE Facet Formation

From the results of the previous section, it is evident that a proper facet and controlled cavity length could induce more pronounced lasing action. Proper industrial settings are often a prerequisite for near-vertical mirror facet formation; to mitigate such a need, RIE-based on-wafer facet fabrication was investigated on the remaining samples as an alternative approach. The test samples had ~3-millimeter-long ridge waveguides and p-pad metallization on top. Facet definition proceeded via photolithography with a positive photoresist, SPR 220-7.0, with 1000 × 30-micrometer patterns periodically arrayed 1100 µm lengthwise/55 µm breadthwise on the sample. The resulting ELO LDs are shown in Figure 4a, with PR covering the ridge and p-pad. The p-pad metal underlying ITO and the SiO_2 isolation layer unprotected by PR were removed using HCl and HF. Then, a Cl_2 RIE was used to form LD facets at the 1000-micrometer cavity ends. Next, the ELO wing LDs were coated with PR once more for protection during scribing. Cuts approximately 150 µm in depth were made between the ELO wing LDs along the guided dicing line shown in Figure 4a from the substrate backside; samples were then separated by pressing. Figure 4b shows SEM images of the RIE facets on the ELO wing LDs. For simplicity of measurement and light collection, the LD sample was divided and left on-wafer; ideally, ELO wing LDs would be lifted from the growth substrate and measured. A commonTi/Al/Ni/Au n-contact (10/50/100/300 nm) was deposited on the substrate backside by e-beam evapo-

ration. Then, the ELO wing LD sample was bonded to a Si carrier coated with Ti/Au/In (10/300/1500 nm). The probing scheme is schematically shown in Figure 4c.

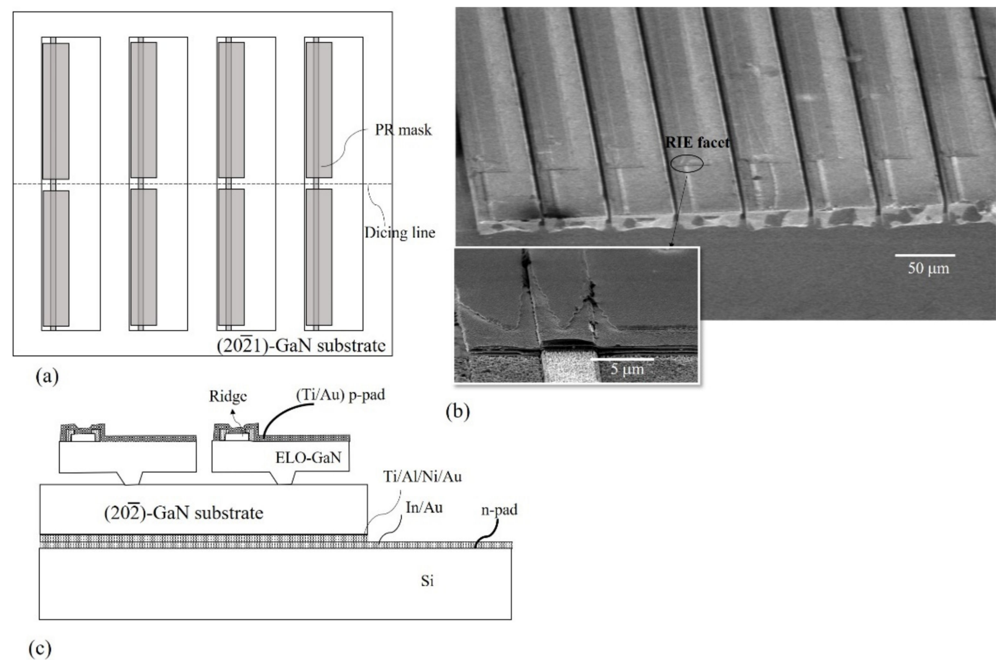

Figure 4. Schematic for on-wafer facet etching: (**a**) PR-masked ELO wing LDs on {20$\bar{2}$1 } semipolar GaN substrate. (**b**) SEM images of on-wafer RIE etched facets of ELO wing LDs. (**c**) Probing scheme for on-wafer RIE facet ELO wing LD.

RIE facet ELO wing LDs were tested by probing the n-pad from the Si carrier and p-pad from the ridge top-side, using a pulsed injection with a pulse width of 0.5 µs and 0.5% duty cycle. Figure 5a shows EL spectra with increasing current injection from 4 kAcm^{-2} to 21 kAcm^{-2}. A lasing peak at 428 nm appeared at 19 kAcm^{-2}, becoming more prominent and intense at 21 kAcm^{-2} and achieving a FWHM of ~0.7 nm. The typical L-I-V curve of a 5 × 1000-micrometer long ELO wing LD is shown in Figure 5b along with an illuminated optical microscope image in the inset. The output power was collected by an integrating sphere placed near the end of one facet. A maximum light output power of ~20 mW was measured from a single-facet at a current density of ~26 kAcm^{-2}. Moreover, the LDs exhibited a threshold current density of ~19 kAcm^{-2}. The slope efficiency was quite low, and we attribute this to strong scattering loss at the facets due to the imperfect RIE etching. We believe further improvements in the growth conditions, as well as the optimization of experimental structure, doping, inclusion of tunnel junctions [33], chemical treatments [34], vertical mirror facet formation [35] and bonding will lead to better L-I-V characteristics. In the past, researchers reported nearly vertical facet formation in the semipolar LDs by Cl_2 gas/Ar-ion chemically assisted ion beam etching (CAIBE) in an Oxford Ion Mill system [35]; as a result, our future investigations will include this method for on-wafer facet formation.

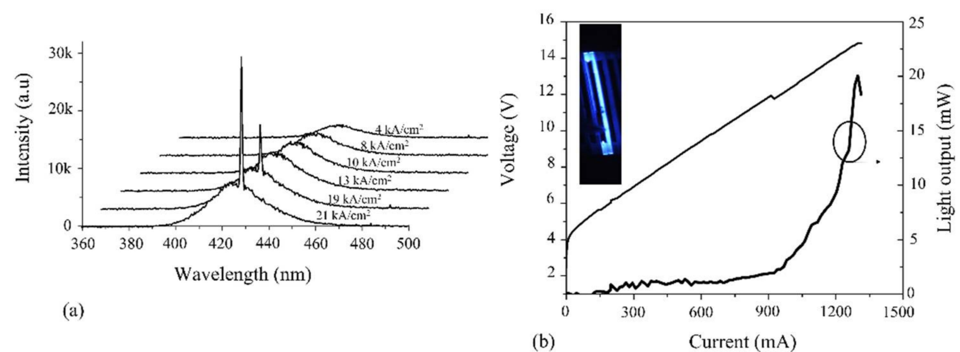

Figure 5. (**a**) Lasing spectrum of an RIE facet ELO wing LD with increasing injection current density (4–21 kAcm^{-2}). (**b**) L-I-V curve of an ELO wing LD with an RIE-formed facet. Inset: Optical microscope image of an illuminated laser device.

4. Conclusions

We have demonstrated pulsed operation in edge-emitting LDs on the reduced-defect ELO wings of semipolar $\{20\bar{2}1\}$ GaN substrate. Handmade facet devices showed spontaneous, LED-like emission, confirming no damage was inflicted to the device layers during mechanical liftoff, and on-wafer facet fabrication achieved lasing at ~428 nm peak emission wavelength. Maximum light output power of 20 mW per facet without facet coatings was measured under pulsed operation from a RIE facet LD. In summary, a proper industrially optimized fractured-facet method could approach conventional cleaved facet yields while recycling the expensive semipolar growth substrate. Alternatively, on-wafer reactive-ion facet etching can also be employed before lifting off LDs from growth substrates. We believe both methods can help overcome the price and material supply issues for semipolar GaN LDs.

5. Patent Applications

i. Takeshi Kamikawa; Srinivas Gandrothula; Hongjian Li; Daniel A. Cohen. Method of removing a substrate. US. Patent US20200194615A1, 18 June 2020.
ii. Takeshi Kamikawa; Srinivas Gandrothula; Hongjian Li; Daniel A. Cohen. Method of removing a substrate. EP. Patent EP3619748A1, 11 March 2020.
iii. Takeshi Kamikawa; Srinivas Gandrothula; Hongjian Li; Daniel A. Cohen. Method for removing substrate. CN. Patent CN110603651A, 20 December 2019.
iv. Takeshi Kamikawa; Srinivas Gandrothula; Hongjian Li; Daniel A. Cohen. How to remove the substrate. JP. Patent JP2020519026A, 25 June 2020.
v. Takeshi Kamikawa; Srinivas Gandrothula; Hongjian Li. Method of removing a substrate with a cleaving technique. US. Patent US20200203228A1, 25 June 2020.
vi. Takeshi Kamikawa; Srinivas Gandrothula; Hongjian Li. Method of removing a substrate with a cleaving technique. EP. Patent EP3682465A1, 22 July 2020.
vii. Takeshi Kamikawa; Srinivas Gandrothula; Hongjian Li. Method for removing substrate by cutting technology. CN. Patent CN111095483A, 1 May 2020.
viii. Takeshi Kamikawa; Srinivas Gandrothula; Hongjian Li. How to remove the substrate using cleavage technique. JP. Patent JP2020534687A, 26 November 2020.
ix. Takeshi Kamikawa; Srinivas Gandrothula; Hongjian Li. Method of fabricating non-polar and semipolar devices using epitaxial lateral overgrowth. US. Patent US20210013365A1, 14 January 2021.
x. Takeshi Kamikawa; Srinivas Gandrothula; Hongjian Li. Method of fabricating non-polar and semipolar devices using epitaxial lateral overgrowth. EP. Patent EP3776672A1, 17 February 2021.
xi. Takeshi Kamikawa; Srinivas Gandrothula; Hongjian Li. Method of fabricating non-polar and semipolar devices using epitaxial lateral overgrowth. CN. Patent CN112219287A, 12 January 2021.

xii. Takeshi Kamikawa; Srinivas Gandrothula; Hongjian Li. Non-polar and semipolar device fabrication method using epitaxial transverse overgrowth. JP. Patent JP2021519743A, 12 August 2021.
xiii. Takeshi Kamikawa; Srinivas Gandrothula. Method for dividing a bar of one or more devices. US. Patent US20210090885A1, 25 March 2021.
xiv. Takeshi Kamikawa; Srinivas Gandrothula. Method for dividing a bar of one or more devices. EP. Patent EP3794632A1, 24 March 2021.
xv. Takeshi Kamikawa; Srinivas Gandrothula. Method for dividing one or more stripes of devices. CN. Patent CN112154533A, 29 December 2020.
xvi. Takeshi Kamikawa; Srinivas Gandrothula. How to split a bar with one or more devices. JP. Patent JP2021525452A, 24 September 2021.
xvii. Srinivas Gandrothula; Takeshi Kamikawa. Method of removing semiconducting layers from a semiconducting substrate. US. Patent US20210242086A1, 5 August 2021.
xviii. Srinivas Gandrothula; Takeshi Kamikawa. Method of removing semiconducting layers from a semiconducting substrate. EP. Patent EP3803980A1, 14 April 2021.
xix. Srinivas Gandrothula; Takeshi Kamikawa. Method for removing semiconducting layer from a semiconductor substrate. CN. Patent CN112204754A, 8 January 2021.
xx. Srinivas Gandrothula; Takeshi Kamikawa. How to remove the semiconductor layer from the semiconductor substrate. JP. Patent JP2021525007A, 16 September 2021.
xxi. Takeshi Kamikawa; Srinivas Gandrothula. Method of obtaining a smooth surface with epitaxial lateral overgrowth. US. Patent WO2020092722A1, 7 May 2020.
xxii. Takeshi Kamikawa; Srinivas Gandrothula. Method of obtaining a smooth surface with epitaxial lateral overgrowth. EP. Patent EP3874544A1, 8 September 2021.
xxiii. Takeshi Kamikawa; Srinivas Gandrothula. Method for obtaining smooth surfaces by epitaxial lateral overgrowth. CN. Patent CN113287205A, 20 August 2021.
xxiv. Takeshi Kamikawa; Srinivas Gandrothula; Masahiro Araki. Method for removal of devices using a trench. US. Patent WO2020150511A1, 23 July 2020.
xxv. Takeshi Kamikawa; Srinivas Gandrothula; Masahiro Araki. Method for removing device using trench. CN. Patent CN113439322A, 24 September 2021.
xxvi. Takeshi Kamikawa; Srinivas Gandrothula. Method for flattening a surface on an epitaxial lateral growth layer. US. Patent WO2020180785A1, 10 September 2020.
xxvii. Takeshi Kamikawa; Masahiro Araki; Srinivas Gandrothula. Substrate for removal of devices using void portions. US. Patent WO2020186205A1, 17 September 2020.
xxviii. Takeshi Kamikawa; Srinivas Gandrothula; Masahiro Araki. Method for removing a bar of one or more devices using supporting plates. US. Patent WO2020186080A1, 17 September 2020.
xxix. Takeshi Kamikawa; Srinivas Gandrothula; Masahiro Araki. Method of fabricating a resonant cavity and distributed Bragg reflector mirrors for a vertical cavity surface emitting laser on a wing of an epitaxial lateral overgrowth region. US. Patent WO2021081308A1, 29 April 2021.
xxx. Takeshi Kamikawa; Masahiro Araki; Srinivas Gandrothula. Method for removing a device using an epitaxial lateral overgrowth technique. US. Patent WO2021212098A1, 21 October 2021.

Author Contributions: Conceptualization, S.G.; investigation, S.G. and H.Z.; data curation, S.G., H.Z. and T.K.; writing—original draft preparation, S.G. and P.S.; writing—review and editing, P.S., R.A., M.S.W. and H.L.; supervision, S.N. and S.P.D.; project administration, S.N. and S.P.D. All authors have read and agreed to the published version of the manuscript.

Funding: This work was supported by the Solid State Lighting and Energy Electronics Center (SSLEEC) at the University of California, Santa Barbara. Authors H.Z., R.A. and M.S.W. would like to thank the partial funding support from DARPA under subcontract No. HR001120C013. A portion of this work was performed in the UCSB Nanofabrication Facility.

Data Availability Statement: The data supporting the findings of this paper are available from the corresponding authors upon reasonable request.

Conflicts of Interest: The authors declare no conflict of interest.

References

1. Nakamura, S.; Senoh, M.; Nagahama, S.; Iwasa, N.; Yamada, T.; Matsushita, T.; Kiyoku, H.; Sugimoto, Y. InGaN-based multiquantum-well-structure laser diodes. *Jpn. J. Appl. Phys.* **1996**, *35*, L74–L76. [CrossRef]
2. Nakamura, S.; Senoh, M.; Nagahama, S.; Iwasa, N.; Yamada, T.; Matsushita, T.; Kiyoku, H.; Sugimoto, Y.; Kozaki, T.; Umemoto, H.; et al. InGaN/GaN/AlGaN-based laser diodes with modulation-doped strained-layer superlattices grown on an epitaxially laterally overgrown GaN substrate. *Appl. Phys. Lett.* **1998**, *72*, 211. [CrossRef]
3. LED Professional. Available online: https://www.led-professional.com/resources-1/articles/professor-shuji-nakamura (accessed on 12 April 2017).
4. Pourhashemi, A.; Farrell, R.M.; Hardy, M.T.; Hsu, P.S.; Kelchner, K.M.; Speck, J.S.; Denbaars, S.P.; Nakamura, S. Pulsed high-power AlGaN-cladding-free blue laser diodes on semipolar (20-2-1) GaN substrates. *Appl. Phys. Lett.* **2013**, *103*, 151112. [CrossRef]
5. Partovi, A.; Peale, D.; Wuttig, M.; Murray, C.A.; Zydzik, G.; Hopkins, L.; Baldwin, K.; Hobson, W.S.; Wynn, J.; Lopata, J.; et al. High-power laser light source for near-field optics and its application to high-density optical data storage. *Appl. Phys. Lett.* **1999**, *75*, 1515–1517. [CrossRef]
6. Morimoto, K.; Kasugai, H.; Takizawa, T.; Yoshida, S.; Yamanaka, K.; Katayama, T.; Okuyama, K.; Shiraishi, S.; Mizuyama, Y. A 30 W Pure Blue Emission with NUV Laser-Diode-Pumped Phosphor for High-Brightness Projectors. *Soc. Inf. Disp. Int. Symp. Dig. Tech.* **2013**, *44*, 832–835. [CrossRef]
7. Denault, K.A.; Cantore, M.; Nakamura, S.; Denbaars, S.; Seshadri, R. Efficient and stable laser-driven white lighting. *AIP Adv.* **2013**, *3*, 072107. [CrossRef]
8. Shen, C.; Ng, T.K.; Leonard, J.T.; Pourhashemi, A.; Nakamura, S.; Denbaars, S.; Speck, J.S.; Alyamani, A.Y.; El-Desouki, M.M.; Ooi, B.S. High-brightness semipolar (2021) blue InGaN/GaN superluminescent diodes for droop-free solid-state lighting and visible-light communications. *Opt. Lett.* **2016**, *41*, 2608–2611. [CrossRef]
9. Murayama, M.; Nakayama, Y.; Yamazaki, K.; Hoshina, Y.; Watanabe, H.; Fuutagawa, N.; Kawanishi, H.; Uemura, T.; Narui, H. Watt-Class Green (530 nm) and Blue (465 nm) Laser Diodes. *Phys. Status Solidi A* **2018**, *215*, 1700513.
10. Masui, S.; Nakatsu, Y.; Kasahara, D.; Nagahama, S.-I. Recent improvement in nitride lasers. In *Gallium Nitride Materials and Devices XII*; International Society for Optics and Photonics: Bellingham, WA, USA, 2017; Volume 10104, p. 101041H. [CrossRef]
11. Avramescu, A.; Hager, T.; Bernhard, S.; Brüderl, G.; Wurm, T.; Somers, A.; Eichler, C.; Vierheilig, C.; Löffler, A.; Ristic, J. High Power Blue and Green Laser Diodes and Their Applications. In Proceedings of the 2014 IEEE Photonics Conference, San Diego, CA, USA, 12–16 October 2014; IEEE: Piscataway, NJ, USA, 2014; pp. 457–458.
12. Chichibu, S.; Azuhata, T.; Sota, T.; Nakamura, S. Spontaneous emission of localized excitons in InGaN single and multi quantum well structures. *Appl. Phys. Lett.* **1996**, *69*, 4188. [CrossRef]
13. Takeuchi, T.; Sota, S.; Katsuragawa, M.; Komori, M.; Takeuchi, H.; Amano, H.; Akasaki, I. Quantum-Confined Stark Effect due to Piezoelectric Fields in GaInN Strained Quantum Wells. *Jpn. J. Appl. Phys.* **1997**, *36*, L382–L385. [CrossRef]
14. Adachi, M. InGaN based green laser diodes on semipolar GaN substrate. *Jpn. J. Appl. Phys.* **2014**, *53*. [CrossRef]
15. Enya, Y.; Yoshizumi, Y.; Kyono, T.; Akita, K.; Ueno, M.; Adachi, M.; Sumitomo, T.; Tokuyama, S.; Ikegami, T.; Katayama, K. 531 nm Green Lasing of InGaN Based Laser Diodes on Semi-Polar {2021} Free-Standing GaN Substrates. *Appl. Phys. Express* **2009**, *2*, 082101. [CrossRef]
16. Lee, C.; Zhang, C.; Cantore, M.; Farrell, R.; Oh, S.H.; Margalith, T.; Speck, J.S.; Nakamura, S.; Bowers, J.E.; DenBaars, S.P. 2.6 GHz high-speed visible light communication of 450 nm GaN laser diode by direct modulation. *Opt. Express* **2015**, *23*, 228–229. [CrossRef]
17. Monavarian, M.; Rashidi, A.; Feezell, D. A Decade of Nonpolar and Semipolar III-Nitrides: A Review of Successes and Challenges. *Phys. Status Solidi A* **2019**, *216*, 1800628. [CrossRef]
18. Hardy, M.T.; Feezell, D.F.; Denbaars, S.; Nakamura, S. Group III-nitride lasers: A materials perspective. *Mater. Today* **2011**, *14*, 408–415. [CrossRef]
19. Zhang, H.; Cohen, D.A.; Chan, P.; Wong, M.S.; Mehari, S.; Becerra, D.L.; Nakamura, S.; Denbaars, S. Continuous-wave operation of a semipolar InGaN distributed-feedback blue laser diode with a first-order indium tin oxide surface grating. *Opt. Lett.* **2019**, *44*, 3106–3109. [CrossRef] [PubMed]
20. Zhang, H.; Daniel, A.C.; Chan, P.; Wong, M.S.; Li, P.; Li, H.; Nakamura, S.; DenBaars, S.P. High performance of a semipolar InGaN laser with a phase-shifted embedded hydrogen silsesquioxane (HSQ) grating. *Opt. Lett.* **2020**, *45*, 5844. [CrossRef] [PubMed]
21. Kamikawa, T.; Gandrothula, S.; Araki, M.; Li, H.; Oliva, V.B.; Wu, F.; Cohen, D.; Speck, J.S.; Denbaars, S.; Nakamura, S. Realization of thin-film m-plane InGaN laser diode fabricated by epitaxial lateral overgrowth and mechanical separation from a reusable growth substrate. *Opt. Express* **2019**, *27*, 24717–24723. [CrossRef] [PubMed]
22. Gandrothula, S.; Kamikawa, T.; Araki, M.; Cohen, D.A.; Speck, J.S.; Nakamura, S.; Denbaars, S. An approach to remove homoepitaxially grown GaN layers by cleavage from the substrate surface. *Appl. Phys. Express* **2020**, *13*, 041003. [CrossRef]
23. Gandrothula, S.; Kamikawa, T.; Speck, J.S.; Nakamura, S.; DenBaars, S.P. Study of surface roughness of lifted-off epitaxial lateral overgrown GaN layers for the n-DBR mirror of a III-nitride vertical-cavity surface emitting laser. *Appl. Phys. Express* **2021**, *14*, 031002. [CrossRef]

24. Gandrothula, S.; Kamikawa, T.; Shapturenka, P.; Anderson, R.; Wong, M.; Zhang, H.; Speck, J.S.; Nakamura, S.; DenBaars, S.P. Optical and electrical characterizations of micro-LEDs grown on lower defect density epitaxial layers. *Appl. Phys. Lett.* **2021**, *119*, 142103. [CrossRef]
25. Kamikawa, T.; Gandrothula, S.; Li, H.; Bonito-Olivia, V.; Wu, F.; Cohen, D.; Speck, J.S.; Denbaars, S.P.; Nakamura, S. New fabrication method of InGaN laser diode by epitaxial lateral overgrowth and cleavable technique from free-standing non- and semi-polar GaN substrate. In *Gallium Nitride Materials and Devices XVI*; International Society for Optics and Photonics: Bellingham, WA, USA, 2021; Volume 11686, p. 116860M.
26. Semiconductor Today. Available online: http://www.semiconductor-today.com/news_items/2020/may/ucsb-150520.shtml (accessed on 15 May 2020).
27. Compound Semiconductor. Available online: https://www.publishing.ninja/V4/page/10557/415/6/1 (accessed on 5 June 2020).
28. Advances in Engineering. Available online: https://advanceseng.com/potential-path-realize-gan-vcsels-epitaxial-lateral-overgrowth/ (accessed on 16 October 2021).
29. Kamei, T.; Kamikawa, T.; Araki, M.; DenBaars, S.P.; Nakamura, S.; Bowers, J.E. Research toward a Heterogeneously Integrated InGaN Laser on Silicon. *Phys. Status Solidi A* **2019**, *217*, 1900770. [CrossRef]
30. Durnev, M.; Omelchenko, A.V.; Yakovlev, E.V.; Evstratov, I.Y.; Karpov, S.Y. Indium incorporation and optical transitions in InGaN bulk materials and quantum wells with arbitrary polarity. *Appl. Phys. Lett.* **2010**, *97*, 051904. [CrossRef]
31. Arefin, R.; You, W.; Ramachandra, S.H.; Hasan, S.M.N.; Jung, H.; Awwad, M.; Arafin, S. Theoretical Analysis of Tunnel-Injected Sub-300 nm AlGaN Laser Diodes. *IEEE J. Quantum Electron.* **2020**, *56*, 2001110. [CrossRef]
32. Wong, M.S.; Melchert, D.; Haggmark, M.; Myers, D.; Lee, C.; Grandrothula, S.; de Vries, M.; Gianola, D.; Begley, M.; Magarlith, T.; et al. Acousto-fluidic assembly of III-nitride micro-light-emitting diodes with magnetic alignment. In *Light-Emitting Devices, Materials, and Applications XXV*; International Society for Optics and Photonics: Bellingham, WA, USA, 2021; Volume 11706, p. 1170607.
33. Hamdy, S.W.; Young, E.C.; Alhassan, A.I.; Becerra, D.L.; Denbaars, S.; Speck, J.S.; Nakamura, S. Efficient tunnel junction contacts for high-power semipolar III-nitride edge-emitting laser diodes. *Opt. Express* **2019**, *27*, 8327–8334. [CrossRef] [PubMed]
34. Wong, M.S.; Back, J.; Hwang, D.; Lee, C.; Wang, J.; Gandrothula, S.; Margalith, T.; Speck, J.S.; Nakamura, S.; DenBaars, S.P. Demonstration of high wall-plug efficiency III-nitride micro-light-emitting diodes with MOCVD-grown tunnel junction contacts using chemical treatments. *Appl. Phys. Express* **2021**, *14*, 086502. [CrossRef]
35. Kuritzky, L.Y.; Becerra, D.L.; Abbas, A.S.; Nedy, J.; Nakamura, S.; Denbaars, S.; Cohen, D.A. Chemically assisted ion beam etching of laser diode facets on nonpolar and semipolar orientations of GaN. *Semicond. Sci. Technol.* **2016**, *31*, 075008. [CrossRef]